Macromolecules
Cite This: Macromolecules 2019, 52, 1663−1670
Article
pubs.acs.org/Macromolecules

# Three-Step Synthesis of a Less-Aggregated Water-Soluble Poly(*p*-phenylene ethynylene) with *Meta* Side Chains via Palladium/Norbornene Cooperative Catalysis

Ki-Young Yoon,[†] Yazhen Xue,[†,‡] and Guangbin Dong*[,†]

[†]Department of Chemistry, University of Chicago, Chicago, Illinois 60637, United States
[‡]College of Chemistry, Peking University, Beijing 100871, China

Supporting Information

**ABSTRACT:** A three-step preparation of a highly water-soluble poly(*p*-phenylene ethynylene) (PPE) from commercially available starting materials is disclosed. The palladium/norbornene-catalyzed AB−C-type polymerization has been developed, which enables installation of two piperazine *meta* side chains concurrently with the construction of the PPE backbone. The capability for double protonation of the piperazine moiety improves water solubility of this material. Compared to the PPE containing *para* side chains, the *meta* side chains reduce interchain aggregation and significantly enhance solubility and fluorescent quantum yields of the polymer.

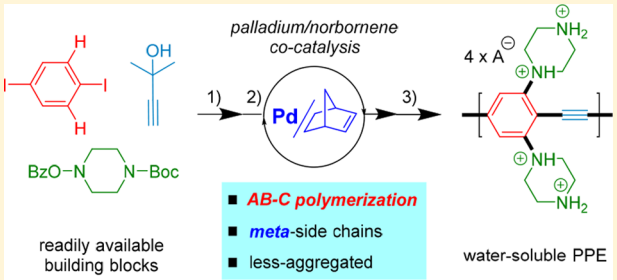


## ■ INTRODUCTION

Poly(*para*-phenylene ethynylene)s (PPE)s feature their remarkable fluorescence properties.[1−7] Hence, many efforts have been particularly made to synthesize water-soluble PPEs for biological[5,8] or sensory applications.[7,9,10] Unfortunately, because of the rigid and hydrophobic nature of the conjugated backbone, water-soluble PPEs have been restrained from broad applications due to polymer aggregation in aqueous medium, which results in fluorescence quenching and low solubility of the material.[11−23] To date, numerous innovated approaches have been demonstrated to circumvent the aggregation issue.[2] For example, one approach was to simply bypass this issue by changing the polymer main chains to less-crystalline backbones, such as poly(*o*-phenylethynylene)s,[17,18] poly(*m*-phenylethynylene)s,[19,20] or bulky arene-containing PPEs.[21,22] On the other hand, the majority of studies have been focused on breaking interchain interactions via modifying side chains of PPEs (Figure 1a). A number of elegant examples have illustrated that side chains, typically with great bulkiness such as ionic dendrimeric units,[12] ionic/polar branched units,[13] or poly(ethylene glycol) units,[14,15] can effectively break aggregation. However, from the synthetic viewpoint, it is not trivial to prepare and introduce those sterically hindered and water-soluble side chains. Hence, it could still be attractive to develop a complementary approach that can alleviate the relatively heavy synthetic demands for preparing water-soluble PPEs.

According to Carnelley's rule, *para*-disubstituted benzenes with $D_{2h}$ symmetry have higher melting points than their less symmetrical *meta* analogues because the *para* isomers intrinsically pack more tightly than the *meta* isomers.[24−26] Thus, we became interested in the regiochemistry effect of side chains on PPE aggregation.[27] The prior examples of preventing aggregation commonly used side chains substituted at the 2,5-positions of the phenylene units (*para* side chains) (Figure 1a);[1−23] in contrast, PPEs possessing *meta* side chains have been unprecedented.[28] We anticipated that placing side chains at the 2,6-positions (*meta* side chains) could effectively break aggregation due to their intrinsically less-ordered packing, which may consequently allow much simpler side chains to be used (Figure 1b). In particular, the piperazine moiety is expected to serve as attractive side chains because, as a common structural motif found in drugs[29−31] and pH-responsive acryloyl-type polymers,[32] piperazine features high water solubility through double protonations of both nitrogen sides ($pK_{a1}$ = 6.3, $pK_{a2}$ = 8.8)[29] under acidic conditions. Herein, we describe our development of a three-step synthesis of a highly water-soluble PPE that contain piperazine *meta* side chains through palladium/norbornene (Pd/NBE)-catalyzed AB−C-type polymerization.

## ■ RESULTS AND DISCUSSION

Pd/NBE cooperative catalysis, also known as the Catellani reaction,[33] has emerged as a useful tool for rapid synthesis of polysubstituted arenes.[34,35] Through forming a unique aryl-norbornyl palladacycle (ANP), an electrophile and a nucleophile are site-selectively coupled at the *ortho* and *ipso* positions, respectively (Figure 2a). In particular, when *ortho*-unsubstituted aryl iodides were used, two new functional

**Received:** December 11, 2018
**Revised:** January 26, 2019
**Published:** February 8, 2019






DOI: 10.1021/acs.macromol.8b02645
Macromolecules 2019, 52, 1663−1670

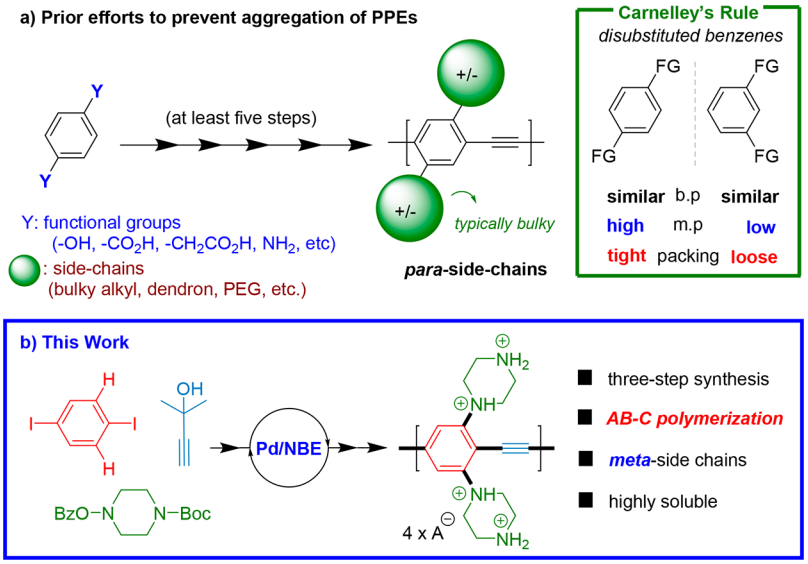


**Figure 1.** Synthetic strategies for less-aggregated water-soluble PPEs.

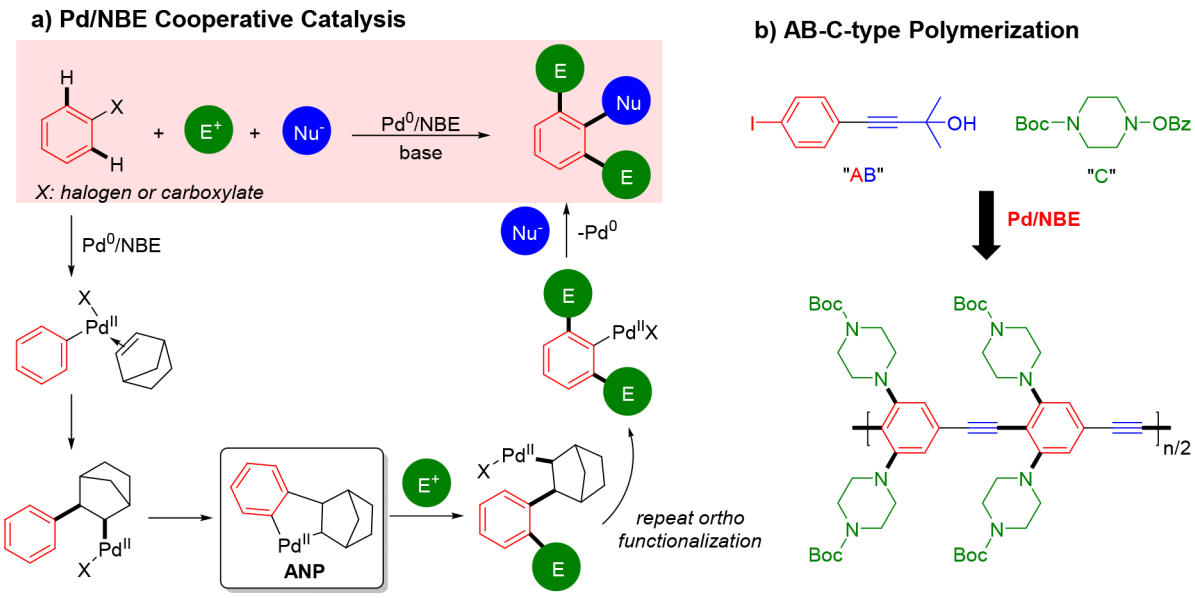


**Figure 2.** Brief illustration of (a) Pd/NBE cooperative catalysis and (b) AB−C-type polymerization.

groups can be introduced at the *ortho* positions simultaneously. Recently, we described our initial efforts of employing the Pd/NBE catalysis in streamlined synthesis of polyfunctionalized aromatic polymers through an $A_2B_2C$-type (*ortho*-amination/*ipso*-alkynylation) polymerization, in which bis-iodoarenes and bis-acetylenes were used as the AA and BB monomers, respectively.[36,37] Given the challenge of preparing PPEs with *meta* side chains in an efficient manner, we were motivated to explore the use of *p*-iodophenylacetylene as a unique AB-type monomer in the Pd/NBE-catalyzed polymerization (Figure 2b). In addition, *N*-benzoyloxy-4-Boc-piperazine will be used as the C-type monomer for introducing piperazine *meta* side chains.[38−42]

A model study was first conducted using 1-iodo-4-(phenylethynyl)benzene (**A**), acetone-protected-phenylacetylene (**B**), and *N*-benzoyloxy-4-Boc-piperazine (**C**) to assess the viability of the AB−C-type Pd/NBE-catalyzed polymerization (Table 1 and Table S1). The major side products came from *ortho*-amination/*ipso*-reduction (**1a**) and the direct Sonogashira coupling (**1b**). The potential alkyne homocoupling product (**1c**) was not observed in any cases, which was a common undesired pathway to introduce defects in PPE preparations.[2,43] After careful optimization, 5 mol % palladium acetate and 12.5 mol % tri(*p*-methoxyphenyl)phosphine were found to be the best precatalyst−ligand combination; ultimately, the desired $\mathbf{M}_{meta}$ compound was afforded in 97% isolated yield (entry 1). Reducing the NBE loading from 200 to 50 mol % slightly decreased the yield of the desired product (entry 2). Decreasing the amount of base or the reaction temperature resulted in more Sonogashira product **1b**, probably because of the negative influence on the *ortho*-C−H activation step (entries 3 and 7). The amount of the *ipso* reduction product **1a** increased at a higher reaction temperature (entry 6); it is likely that the elimination of benzoate from **C** may be accelerated at the higher temperature, which generated the corresponding imine or enamine serving as the reductant.[38] It is noteworthy


DOI: 10.1021/acs.macromol.8b02645
Macromolecules 2019, 52, 1663−1670

**Table 1. Selected Optimization of the Model Reaction**

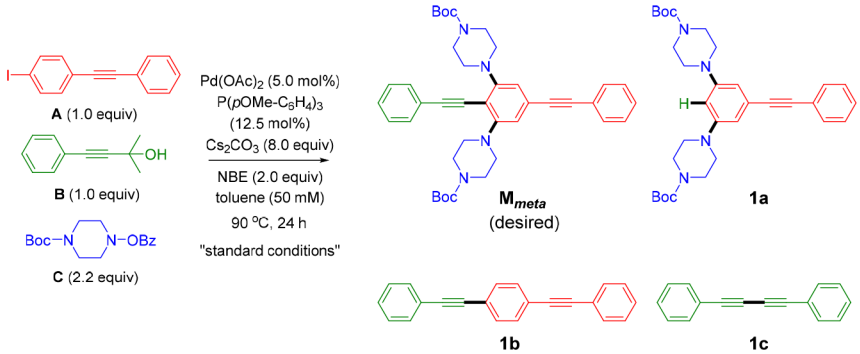


| entry | change from the "standard conditions" | yield (%) ($\mathbf{M}_{meta}$[a]:**1a**[a]:**1b**[b]:**1c**[b]) |
|---|---|---|
| 1 | none | >95 (97[c]):<5:0:0 |
| 2 | 0.5 equiv NBE | 95:<5:trace:0 |
| 3 | 4.0 equiv $Cs_2CO_3$ | 90:<5:3:0 |
| 4 | 10 mol % P(*p*OMe-$C_6H_4$)$_3$ | 93:5:trace:0 |
| 5 | 15 mol % P(*p*OMe-$C_6H_4$)$_3$ | 85:5:6:0 |
| 6 | 100 °C | 93:5:trace:0 |
| 7 | 80 °C | 88:<5:3:0 |

[a]Determined by $^1$H NMR and GC with 1,3,5-trimethoxbenzene as the internal standard. [b]Determined by GC with 1,3,5-trimethoxbenzene as the internal standard. [c]Isolated yield.

**Scheme 1. Synthesis of the Water-Soluble PPE $PE_{meta}$**

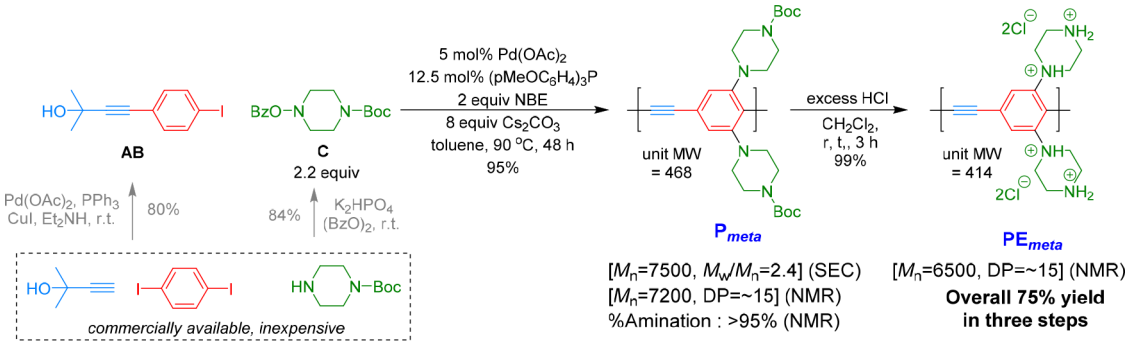


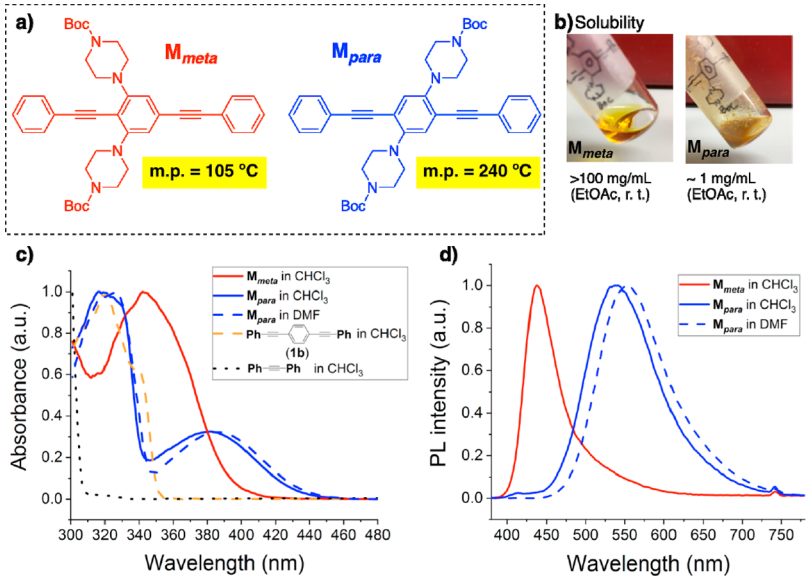


**Figure 3.** (a) Chemical structures of $\mathbf{M}_{meta}$ and $\mathbf{M}_{para}$. The differences of $\mathbf{M}_{meta}$ (red) and $\mathbf{M}_{para}$ (blue) in terms of (b) solubility, (c) UV/vis absorption (normalized), and (d) fluorescence (normalized, ex 370 nm). The absorption and emission spectra were obtained with a solution of 5 $\mu$M.



DOI: 10.1021/acs.macromol.8b02645
*Macromolecules* 2019, 52, 1663−1670

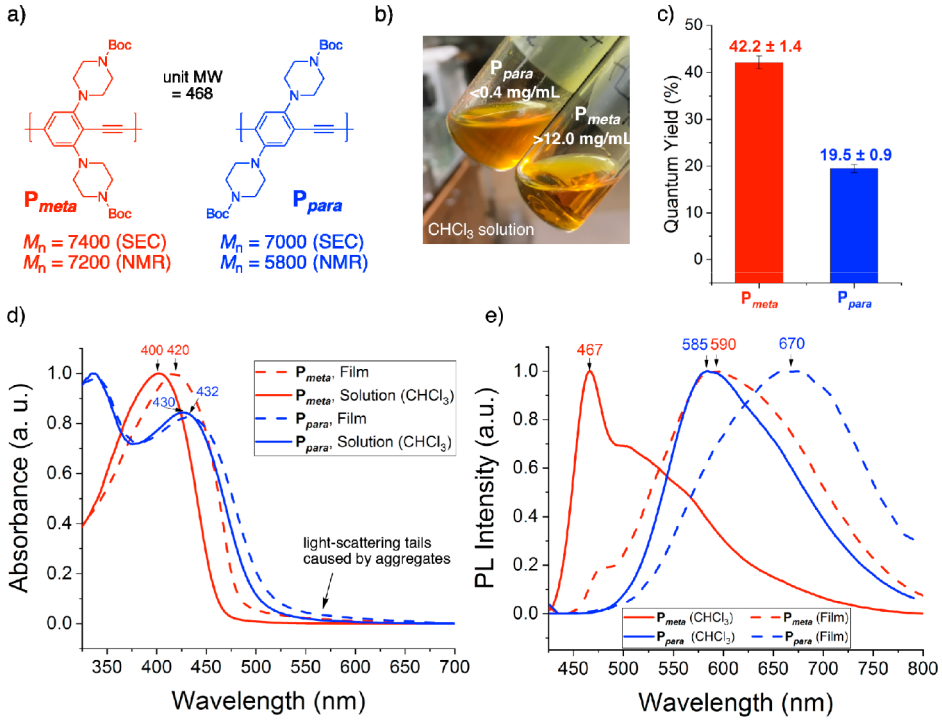


**Figure 4.** (a) Chemical structures of $\mathbf{P}_{meta}$ and $\mathbf{P}_{para}$. The differences of $\mathbf{P}_{meta}$ (red) and $\mathbf{P}_{para}$ (blue) in terms of (b) solubility, (c) fluorescence quantum yields, (d) UV/vis absorption (normalized), and (e) fluorescence (normalized, ex 410 nm). The absorption and emission spectra were obtained with a solution of 5 $\mu$M (based on the molar mass of the repeating unit). The relative quantum yields were measured three times based on quinine sulfate (1 N $H_2SO_4$) and three times based on 9,10-diphenylanthracene in cyclohexane as internal standards.

that the reaction profile relied heavily on the ratio of the palladium catalyst and the ligand (entries 4 and 5).

With the optimal reaction conditions in hand, the AB−C polymerization was investigated (Scheme 1). The **AB** monomer was prepared directly through Sonogashira coupling of commercially available 1,4-diiodobenzene and 2-methyl-3-butyn-2-ol. The polymerization between **AB** and **C** monomers proceeded smoothly to afford $\mathbf{PE}_{meta}$ in 95% yield with $M_n$ = 7500 and $M_w/M_n$ = 2.4 (based on polystyrene standards in chloroform SEC), which contains two piperazine *meta* side chains in each repeating unit. The degree of polymerization was 15 based upon the end-group analysis by $^1$H NMR (Figure S1). The subsequent deprotection of the Boc group with excess HCl provided conjugated polyelectrolyte $\mathbf{PE}_{meta}$ in nearly a quantitative yield. Hence, this approach allows for a three-step synthesis of a water-soluble PPE with *meta* side chains in a 75% overall yield.

Efforts were next put forth to understand the properties of this new material. First, to examine whether the phenylacetylene moiety containing two piperazine units would follow Carnelley's rule, model substrates $\mathbf{M}_{meta}$ and $\mathbf{M}_{para}$ were synthesized (Figure 3a; see the Supporting Information for their syntheses). The melting point of the less symmetrical $\mathbf{M}_{meta}$ was substantially lower than that of $\mathbf{M}_{para}$ (105 °C vs 240 °C), indicating that the phenylacetylene possessing *meta* side chains is indeed less packed. The loosely packed $\mathbf{M}_{meta}$ isomer relative to $\mathbf{M}_{para}$ was also supported by single crystal X-ray diffraction (Figure S2). Coherently, $\mathbf{M}_{meta}$ was found over 100 times more soluble than $\mathbf{M}_{para}$ in ethyl acetate at room temperature (Figure 3b and Figure S4).

In addition, the two regioisomers showed different electronic properties. Two distinct transitions at 320 and 380 nm were displayed by the absorption spectrum of $\mathbf{M}_{para}$ in chloroform, and they red-shifted in more polar solvent such as DMF (Figure 3c and Figure S5). This behavior indicated the presence of intramolecular charge-transfer (ICT) character, implying the sufficient electron-donating capability of the electron-rich phenylenes containing the *p*-piperazine units to form donor−acceptor pairs with the ethynylene moieties via the ICT process.[44,45] In contrast, $\mathbf{M}_{meta}$ featured a single transition, where the ICT process was hampered because the oxidized form of $\mathbf{M}_{meta}$ would form less stable quinoidal resonance structures than the one of $\mathbf{M}_{para}$.[46,47] Nevertheless, $\mathbf{M}_{meta}$ exhibited a more red-shifted absorption than the corresponding unsubstituted compound **1b**, which is likely caused by increased energy of the highest-occupied molecular orbital in this conjugated system. Similar to the previous reports,[48−50] the broad absorption spectra of both isomers were attributed to twisting of the phenyl rings from the coplanar geometry as shown in the crystal structures (Figure S3). The fluorescence spectrum of $\mathbf{M}_{para}$, compared to that of $\mathbf{M}_{meta}$, was significantly broadened, accompanied by a larger Stokes shift (Figure 3d). The radiative lifetime ($\tau_{rad}$) for $\mathbf{M}_{para}$ is significantly longer than the value for $\mathbf{M}_{meta}$ ($\tau_{rad}$ = 29 ns for $\mathbf{M}_{para}$ and $\tau_{rad}$ = 3.2 ns for $\mathbf{M}_{meta}$), indicating a large long-lived contribution from the ICT state (Table S2).[51] These fluorescence data suggested that the structural difference between the ground and excited states were greater in the case of $\mathbf{M}_{para}$ due to the more planar structure of $\mathbf{M}_{para}$ at the excited state through the ICT process and/or the corresponding interchain interaction to form excimer-like excited states.[23,52−54] All these observations concluded that the simple alteration of substitution positions dramatically influenced the packing/aggregation pattern of the model compounds.

To investigate the regiochemistry effect of side chains on polymer aggregations, the PPE that contains piperazine *para*


DOI: 10.1021/acs.macromol.8b02645
Macromolecules 2019, 52, 1663−1670

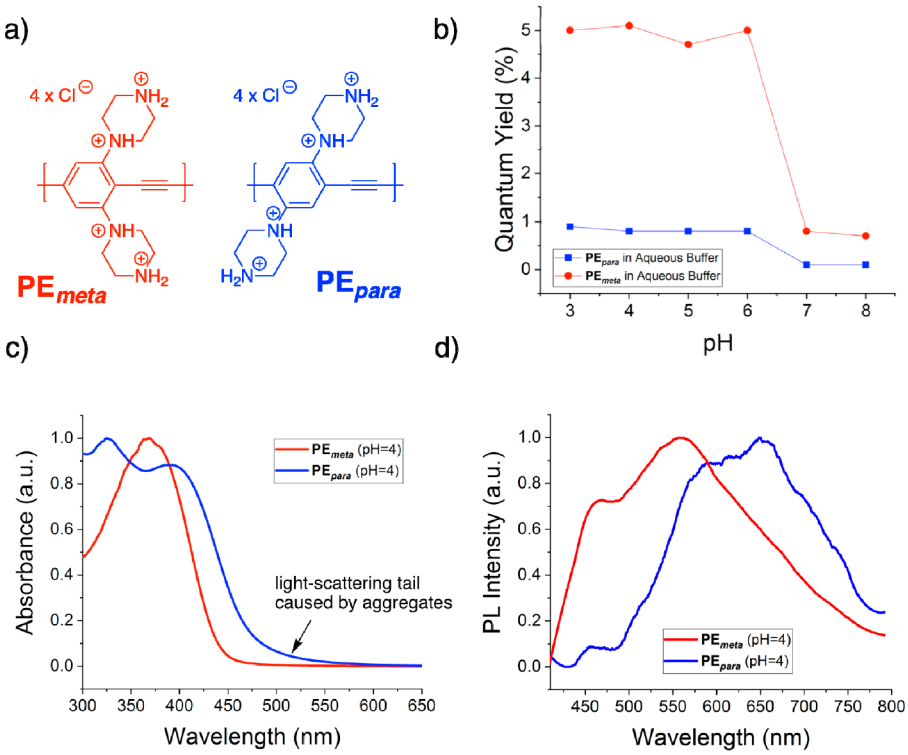


**Figure 5.** (a) Chemical structures of $\mathbf{PE}_{meta}$ and $\mathbf{PE}_{para}$. The differences of $\mathbf{PE}_{meta}$ (red) and $\mathbf{PE}_{para}$ (blue) in terms of (b) fluorescence quantum yields, (c) UV/vis absorption (normalized), and (d) fluorescence (normalized, ex 410 nm). The absorption and emission spectra were obtained with a solution of 5 $\mu$M (based on the molar mass of the repeating unit). The relative quantum yields were measured based on quinine sulfate (1 N $H_2SO_4$) and based on 9,10-diphenylanthracene in cyclohexane as internal standards.

side chains with a comparable molecular weight ($\mathbf{P}_{para}$) was prepared by conventional Sonogashira polymerization of the monomer with preinstalled side chains (Figure 4; see the Supporting Information for its synthesis). Compared to $\mathbf{P}_{meta}$, $\mathbf{P}_{para}$ featured the relatively large discrepancy between $M_n$s by SEC and $^1$H NMR analyses (Figure 4a). This indicated the relatively high hydrodynamic volume of $\mathbf{P}_{para}$, inferring that $\mathbf{P}_{para}$ could be more rigid than $\mathbf{P}_{meta}$. With regard to the optical property (Figures 4d and 4e), $\mathbf{P}_{meta}$ exhibited a strong absorption band in blue region ($\lambda_{max}$ = 400 nm) along with a strong blue fluorescence ($\lambda_{max}$ = 467 nm) in chloroform. In film, $\mathbf{P}_{meta}$ displayed the absorption with the bathochromic shift of 20 nm from the maximum absorption in solution. In stark contrast to the emission of $\mathbf{P}_{meta}$ in solution, the broad green fluorescence with a large Stokes shift of 170 nm was observed from the sample in film state. This suggested that a conformational change from the twisted absorbing ground state to the planar emitting excited state facilitated an excimer-like excited state arising from interchain $\pi$−$\pi$ stacking in the aggregated state.[52−55] Nonetheless, the slight emission peak at ∼470 nm coming from the nonaggregated form was still observed in film.[55] The absorption spectra of $\mathbf{P}_{para}$ displayed two distinct transitions similar to the one of $\mathbf{M}_{para}$, which is caused by the ICT (Figure S5). Note that $\mathbf{P}_{para}$ showed a more significant light-scattering tail in the longer wavelength than $\mathbf{P}_{meta}$ even in solution, which is likely caused by a more aggregated state.[56] In addition, the fluorescence spectra of $\mathbf{P}_{para}$ in solution showed the broad emission with a large Stokes shift; this implied that the interchain interaction of $\mathbf{P}_{para}$ in solution was as large as that of $\mathbf{P}_{meta}$ in the aggregated state, which could be due to the packable nature of the more symmetrical $\mathbf{P}_{para}$ as well as the more planar excited state via the ICT.[24,44,57] $\mathbf{P}_{para}$ in film exhibited further red-shifted emission, without a corresponding change in the absorption spectrum compared to the one in solution. It is therefore anticipated that $\mathbf{P}_{para}$ involved a larger structural change from the ground to the excited states than $\mathbf{P}_{meta}$, which consequently resulted in the longer fluorescence/radiative lifetime than $\mathbf{P}_{meta}$ in solution (Table S2) due to the smaller overlap of the vibronic wave functions of the ground and excited states.[44,51,57] Overall, it can be inferred that the rigid $\mathbf{P}_{para}$ was more likely to aggregate. Correspondingly, $\mathbf{P}_{meta}$ is over 30 times more soluble than $\mathbf{P}_{para}$ in chloroform (>12.0 mg/mL vs 0.4 mg/mL) (Figure 4b). Less aggregated $\mathbf{P}_{meta}$ displayed a twice higher fluorescence quantum yield than $\mathbf{P}_{para}$ (42.2% vs 19.5%) in chloroform solution (Figure 4c). As expected, fluorescence was quenched when aggregation was forced to take place by adding poor solvents such as methanol (Figure S6).

Water-soluble PPEs, $\mathbf{PE}_{meta}$ and $\mathbf{PE}_{para}$, showed the same aggregation trend. The solubility of $\mathbf{PE}_{meta}$ in water was significantly higher than that of $\mathbf{PE}_{para}$ (>80 mg/mL vs 7 mg/mL in distilled water, Figure S4). Interestingly, the solubility of $\mathbf{PE}_{meta}$ and $\mathbf{PE}_{para}$ in water was higher than that of $\mathbf{P}_{meta}$ and $\mathbf{P}_{para}$ in organic solvents, which indeed indicated high solubilizing capability of doubly protonated piperazine groups. Because the p$K_a$ value of the aniline nitrogen of phenylpiperazine moiety is 6.3,[29] $\mathbf{PE}_{meta}$ was more soluble in acidic aqueous buffers than water and was less soluble in neutral/basic buffers than water.[58] The absorption spectra of $\mathbf{PE}_{meta}$ and $\mathbf{PE}_{para}$ in pH = 4 acidic aqueous buffer showed transitions similar to their precursors $\mathbf{P}_{meta}$ and $\mathbf{P}_{para}$, respectively, except that these peaks were blue-shifted (Figure 5c).[13] $\mathbf{PE}_{para}$ in solution exhibited analogous fluorescence patterns to $\mathbf{P}_{para}$ in film, which illustrated that $\mathbf{PE}_{para}$ was situated in aqueous


DOI: 10.1021/acs.macromol.8b02645
Macromolecules 2019, 52, 1663−1670

medium closer to the aggregated state (Figure 5d and Figure S7). The aggregating nature of water-soluble PPEs relative to their precursors in solution was expected due to the hydrophobic conjugated backbone in water. It is also likely that the flattened backbone of $\mathbf{PE}_{para}$ promoted by the enhanced ICT in the polar medium facilitated aggregation. In contrast, introducing *meta* side chains to the conjugated main chain attenuated the polymer aggregation, and thus $\mathbf{PE}_{meta}$ in solution showed the major emission peak at 560 nm corresponding to the aggregated state, concurrently with a prominent shoulder at 455 nm corresponding to the nonaggregated state.[55] As a control experiment, the emission peak at 455 nm disappeared in pH = 8 aqueous buffer in addition to the red-shifted absorption with light-scattering tails (Figure S8), further implying that the presence of the protonated aniline moieties might be crucial to break the aggregation.[56,58] Accordingly, the fluorescence quantum yield of $\mathbf{PE}_{meta}$ was significantly decreased from 5.0% to <1.0% at pH higher than 7 likely due to aggregation-caused fluorescence quenching (Figure 5b). Interestingly, the fluorescence of $\mathbf{PE}_{meta}$ was found significantly enhanced upon addition of 70 vol % methanol to pH = 4 aqueous buffer, which enhanced the fluorescence quantum yield from 5.0% to 18.3% (Figure S9). One explanation is that the aggregation was broken in such a cosolvent system, as the greenish emission of $\mathbf{PE}_{meta}$ was blue-shifted after addition of methanol, accompanied by a clear strength enhancement of the nonaggregated emission peak at 455 nm. The exact reaction for the deaggregation of polymers remains unclear and is currently under investigation.

## ■ CONCLUSION

In summary, we disclosed a simple three-step preparation of a highly water-soluble PPE from commercially available starting materials. Through developing a Pd/NBE-catalyzed AB−C-type polymerization, piperazine *meta* side chains were installed concurrently with the construction of the PPE backbone. The capability for double protonation of the piperazine moiety was one key factor for high water solubility of this material. On the other hand, compared to the corresponding PPE containing piperazine *para* side chains, the one possessing *meta* side chains was less aggregated, was much more soluble, and gave a higher fluorescent quantum yield. This observation suggests that the substitution pattern of side chains alone can significantly affect polymer properties, which should have a broad implication beyond this work. Efforts in exploring the utility of this densely charged PPE material are ongoing.

## ■ ASSOCIATED CONTENT

### Supporting Information

The Supporting Information is available free of charge on the ACS Publications website at DOI: 10.1021/acs.macromol.8b02645.

Experimental details; Figures S1−S9 and Tables S1−S3 (PDF)

X-ray crystallographic data of the model substrate $\mathbf{M}_{para}$ (CIF)

## ■ AUTHOR INFORMATION


### Corresponding Author

*E-mail: gbdong@uchicago.edu.

### ORCID

Ki-Young Yoon: 0000-0003-3257-6103

Guangbin Dong: 0000-0003-1331-6015


### Notes

The authors declare no competing financial interest.

## ■ ACKNOWLEDGMENTS

The University of Chicago and NSF (CHE 1707399) are acknowledged for research support. K.-Y.Y. thanks the Kwanjeong Educational Foundation for a graduate fellowship. Mr. Jianchun Wang is thanked for checking the experiments. We acknowledge the MRSEC Shared User Facilities at the University of Chicago (NSF DMR-1420709).

## ■ REFERENCES


(1) Bunz, U. H. F. Poly(aryleneethynylene)s: Syntheses, Properties, Structures, and Applications. *Chem. Rev.* **2000**, *100*, 1605−1644.

(2) Bunz, U. H. F. Poly(aryleneethynylene)s. *Macromol. Rapid Commun.* **2009**, *30*, 772−805.

(3) Jiang, H.; Taranekar, P.; Reynolds, J. R.; Schanze, K. S. Conjugated Polyelectrolytes: Synthesis, Photophysics, and Applications. *Angew. Chem., Int. Ed.* **2009**, *48*, 4300−4316.

(4) Liu, Y.; Ogawa, K.; Schanze, K. S. Conjugated Polyelectrolytes as Fluorescent Sensors. *J. Photochem. Photobiol., C* **2009**, *10*, 173−190.

(5) Zhu, C.; Liu, L.; Yang, Q.; Lv, F.; Wang, S. Water-Soluble Conjugated Polymers for Imaging, Diagnosis, and Therapy. *Chem. Rev.* **2012**, *112*, 4687−4735.

(6) Duarte, A.; Pu, K.-Y.; Liu, B.; Bazan, G. C. Recent Advances in Conjugated Polyelectrolytes for Emerging Optoelectronic Applications. *Chem. Mater.* **2011**, *23*, 501−515.

(7) Thomas, S. W., III; Joly, G. D.; Swager, T. M. Chemical Sensors Based on Amplifying Fluorescent Conjugated Polymers. *Chem. Rev.* **2007**, *107*, 1339−1386.

(8) Wosnick, J. H.; Mello, C. M.; Swager, T. M. Synthesis and Application of Poly(phenylene ethynylene)s for Bioconjugation: A Conjugated Polymer-Based Fluorogenic Probe for Proteases. *J. Am. Chem. Soc.* **2005**, *127*, 3400−3405.

(9) Zhao, X.; Liu, Y.; Schanze, K. S. A Conjugated Polyelectrolyte-Based Fluorescence Sensor for Pyrophosphate. *Chem. Commun.* **2007**, 2914−2916.

(10) Tan, C.; Atas, E.; Müller, J. G.; Pinto, M. R.; Kleiman, V. D.; Schanze, K. S. Amplified Quenching of a Conjugated Polyelectrolyte by Cyanine Dyes. *J. Am. Chem. Soc.* **2004**, *126*, 13685−13694.

(11) Deans, R.; Kim, J.; Machacek, M. R.; Swager, T. M. A Poly(*p*-phenyleneethynylene) with a Highly Emissive Aggregated Phase. *J. Am. Chem. Soc.* **2000**, *122*, 8565−8566.

(12) Jiang, D.-L.; Choi, C.-K.; Honda, K.; Li, W.-S.; Yuzawa, T.; Aida, T. Photosensitized Hydrogen Evolution From Water Using Conjugated Polymers Wrapped in Dendrimeric Electrolytes. *J. Am. Chem. Soc.* **2004**, *126*, 12084−12089.

(13) Lee, S. H.; Kömürlü, S.; Zhao, X.; Jiang, H.; Moriena, G.; Kleiman, V. D.; Schanze, K. S. Water-Soluble Conjugated Polyelectrolytes with Branched Polyionic Side Chains. *Macromolecules* **2011**, *44*, 4742−4751.

(14) Lee, K.; Kim, H.-J.; Kim, J. Design Principle of Conjugated Polyelectrolytes to Make Them Water-Soluble and Highly Emissive. *Adv. Funct. Mater.* **2012**, *22*, 1076−1086.

(15) Khan, A.; Müller, S.; Hecht, S. Practical Synthesis of an Amphiphilic, Non-Ionic Poly(*para*-phenyleneethynylene) Derivative with a Remarkable Quantum Yield in Water. *Chem. Commun.* **2005**, 584−586.

(16) Koenen, J.-M.; Zhu, X.; Pan, Z.; Feng, F.; Yang, J.; Schanze, K. S. Enhanced Fluorescence Properties of Poly(phenylene ethynylene)-Conjugated Polyelectrolytes Designed to Avoid Aggregation. *ACS Macro Lett.* **2014**, *3*, 405−409.

(17) Jones, T. V.; Blatchly, R. A.; Tew, G. N. Synthesis of Alkoxy-Substituted *ortho*-Phenylene Ethynylene Oligomers. *Org. Lett.* **2003**, *5*, 3297−3299.

(18) Khan, A.; Hecht, S. Poly(*ortho*-phenylene ethynylene)s: Synthetic Accessibility and Optical Properties. *J. Polym. Sci., Part A: Polym. Chem.* **2006**, *44*, 1619−1627.
(19) Arnt, L.; Tew, G. N. New Poly(phenyleneethynylene)s with Cationic, Facially Amphiphilic Structures. *J. Am. Chem. Soc.* **2002**, *124*, 7664−7665.
(20) Stone, M. T.; Moore, J. S. A Water-Soluble *m*-Phenylene Ethynylene Foldamer. *Org. Lett.* **2004**, *6*, 469−472.
(21) Swager, T. M. Iptycenes in the Design of High Performance Polymers. *Acc. Chem. Res.* **2008**, *41*, 1181−1189.
(22) Pschirer, N. G.; Vaughn, M. E.; Dong, Y. B.; zur Loye, H.-C.; Bunz, U. H. F. Novel Liquid-Crystalline PPE-Naphthalene Copolymers Displaying Blue Solid-State Fluorescence. *Chem. Commun.* **2000**, 85−86.
(23) Tan, C.; Pinto, M. R.; Schanze, K. S. Photophysics, Aggregation and Amplified Quenching of a Water-Soluble Poly(phenylene ethynylene). *Chem. Commun.* **2002**, 446−447.
(24) Brown, R. J. C.; Brown, R. F. C. Melting Point and Molecular Symmetry. *J. Chem. Educ.* **2000**, *77*, 724−731.
(25) Gavezzotti, A. Molecular Symmetry, Melting Temperatures and Melting Enthalpies of Substituted Benzenes and Naphthalenes. *J. Chem. Soc., Perkin Trans. 2* **1995**, *2*, 1399−1404.
(26) Boese, R.; Kirchner, M. T.; Dunitz, J. D.; Filippini, G.; Gavezzotti, A. Solid-State Behaviour of the Dichlorobenzenes: Actual, Semi-Virtual and Virtual Crystallography. *Helv. Chim. Acta* **2001**, *84*, 1561−1577.
(27) Lei, T.; Wang, J.-Y.; Pei, J. Roles of Flexible Chains in Organic Semiconducting Materials. *Chem. Mater.* **2014**, *26*, 594−603.
(28) For a seminal work in synthesis of soluble graphene nanoribbons containing aryl *meta* side chains, see: Yang, W.; Lucotti, A.; Tommasini, M.; Chalifoux, W. A. Bottom-Up Synthesis of Soluble and Narrow Graphene Nanoribbons Using Alkyne Benzannulations. *J. Am. Chem. Soc.* **2016**, *138*, 9137−9144.
(29) Lin, C.-E.; Deng, Y.-J.; Liao, W.-S.; Sun, S.-W.; Lin, W.-Y.; Chen, C.-C. Electrophoretic Behavior and pKa Determination of Quinolones with a Piperazinyl Substituent by Capillary Zone Electrophoresis. *J. Chromatogr., A* **2004**, *1051*, 283−290.
(30) Marvanova, P.; Padrtova, T.; Odehnalova, K.; Hosik, O.; Oravec, M.; Mokry, P. Synthesis and Determination of Physicochemical Properties of New 3-(4-Arylpiperazin-1-yl)-2-Hydroxypropyl 4-Alkoxyethoxybenzoates. *Molecules* **2016**, *21*, 1682.
(31) Tahirovic, Y. A.; Truax, V. M.; Wilson, R. J.; Jecs, E.; Nguyen, H. H.; Miller, E. J.; Kim, M. B.; Kuo, K. M.; Wang, T.; Sum, C. S.; Cvijic, M. E.; Schroeder, G. M.; Wilson, L. J.; Liotta, D. C. Discovery of N-Alkyl Piperazine Side Chain Based CXCR4 Antagonists with Improved Drug-Like Properties. *ACS Med. Chem. Lett.* **2018**, *9*, 446−451.
(32) Kocak, G.; Tuncer, C.; Bütün, V. pH-Responsive Polymers. *Polym. Chem.* **2017**, *8*, 144−176.
(33) Catellani, M.; Frignani, F.; Rangoni, A. A Complex Catalytic Cycle Leading to a Regioselective Synthesis *o*,*o*′-Disubstituted Vinylarenes. *Angew. Chem., Int. Ed. Engl.* **1997**, *36*, 119−122.
(34) Della Ca, N.; Fontana, M.; Motti, E.; Catellani, M. Pd/Norbornene: a Winning Combination for Selective Aromatic Functionalization via C−H Bond Activation. *Acc. Chem. Res.* **2016**, *49*, 1389−1400.
(35) Ye, J.; Lautens, M. Palladium-Catalysed Norbornene-Mediated C−H Functionalization of Arenes. *Nat. Chem.* **2015**, *7*, 863−870.
(36) Yoon, K.-Y.; Dong, G. Modular *in Situ* Functionalization Strategy: Multicomponent Polymerization by Palladium/Norbornene Cooperative Catalysis. *Angew. Chem., Int. Ed.* **2018**, *57*, 8592−8596.
(37) For an elegant seminal work on ladder polymer synthesis by Pd-catalyzed arene−norbornene annulation, see: Liu, S.; Jin, Z.; Teo, Y. C.; Xia, Y. Efficient Synthesis of Rigid Ladder Polymers via Palladium Catalyzed Annulation. *J. Am. Chem. Soc.* **2014**, *136*, 17434−17437.
(38) Dong, Z.; Dong, G. Ortho vs Ipso: Site-Selective Pd and Norbornene-Catalyzed Arene C−H Amination Using Aryl Halides. *J. Am. Chem. Soc.* **2013**, *135*, 18350−18353.
(39) Sun, F.; Gu, Z. Decarboxylative Alkynyl Termination of Palladium-Catalyzed Catellani Reaction: A Facile Synthesis of α-Alkynyl Anilines via *Ortho* C−H Amination and Alkynylation. *Org. Lett.* **2015**, *17*, 2222−2225.
(40) Pan, S.; Ma, X.; Zhong, D.; Chen, W.; Liu, M.; Wu, H. Palladium-Catalyzed One-Pot Consecutive Amination and Sonogashira Coupling for Selective Synthesis of 2-Alkynylanilines. *Adv. Synth. Catal.* **2015**, *357*, 3052−3056.
(41) Dong, Z.; Lu, G.; Wang, J.; Liu, P.; Dong, G. Modular *ipso*/*ortho* Difunctionalization of Aryl Bromides via Palladium/Norbornene Cooperative Catalysis. *J. Am. Chem. Soc.* **2018**, *140*, 8551−8562.
(42) Wang, J.; Li, R.; Dong, Z.; Liu, P.; Dong, G. Complementary Site-Selectivity in Arene Functionalization Enabled by Overcoming the *ortho* Constraint in Palladium/Norbornene Catalysis. *Nat. Chem.* **2018**, *10*, 866−872.
(43) Kloppenburg, L.; Jones, D.; Bunz, U. H. F. High Molecular Weight Poly(*p*-phenyleneethynylene)s by Alkyne Metathesis Utilizing "Instant" Catalysts: A Synthetic Study. *Macromolecules* **1999**, *32*, 4194−4203.
(44) Thomas, S. W., III; Swager, T. M. Synthesis and Optical Properties of Simple Amine-Containing Conjugated Polymers. *Macromolecules* **2005**, *38*, 2716−2721.
(45) Moroni, M.; Le Moigne, J.; Pham, T. A.; Bigot, J. Y. Rigid Rod Conjugated Polymers for Nonlinear Optics. 3. Intramolecular H Bond Effects on Poly(phenyleneethynylene) Chains. *Macromolecules* **1997**, *30*, 1964−1972.
(46) Glicksman, R. Investigation of the Electrochemical Characteristics of Organic Compounds: VI. Aromatic Hydroxy, Aromatic Amine, and Aminophenol Compounds. *J. Electrochem. Soc.* **1961**, *108*, 1−6.
(47) Enache, T. A.; Oliveira-Brett, A. M. Phenol and *para*-Substituted Phenols Electrochemical Oxidation Pathways. *J. Electroanal. Chem.* **2011**, *655*, 9−16.
(48) Sluch, M. I.; Godt, A.; Bunz, U. H. F.; Berg, M. A. Excited-State Dynamics of Oligo(*p*-phenyleneethynylene): Quadratic Coupling and Torsional Motions. *J. Am. Chem. Soc.* **2001**, *123*, 6447−6448.
(49) Levitus, M.; Schmieder, K.; Ricks, H.; Shimizu, K. D.; Bunz, U. H. F.; Garcia-Garibay, M. A. Steps to Demarcate the Effects of Chromophore Aggregation and Planarization in Poly(phenyleneethynylene)s. 1. Rotationally Interrupted Conjugation in the Excited States of 1,4-Bis(phenylethynyl)benzene. *J. Am. Chem. Soc.* **2001**, *123*, 4259−4265.
(50) Levitus, M.; Zepeda, G.; Dang, H.; Godinez, C.; Khuong, T.-A. V.; Schmieder, K.; Garcia-Garibay, M. A. Steps to Demarcate the Effects of Chromophore Aggregation and Planarization in Poly(phenyleneethynylene)s. 2. The Photophysics of 1,4-Diethynyl-2-fluorobenzene in Solution and in Crystals. *J. Org. Chem.* **2001**, *66*, 3188−3195.
(51) Morris, W. A.; Kolpaczynska, M.; Fraser, C. L. Effects of α-Substitution on Mechanochromic Luminescence and Aggregation-Induced Emission of Difluoroboron β-Diketonate Dyes. *J. Phys. Chem. C* **2016**, *120*, 22539−22548.
(52) Huang, W. Y.; Gao, W.; Kwei, T. K.; Okamoto, Y. Synthesis and Characterization of Poly(alkyl-substituted *p*-phenylene ethynylene)s. *Macromolecules* **2001**, *34*, 1570−1578.
(53) Pinto, M. R.; Kristal, B. M.; Schanze, K. S. A Water-Soluble Poly(phenylene ethynylene) with Pendant Phosphonate Groups. Synthesis, Photophysics, and Layer-by-layer Self-Assembled Films. *Langmuir* **2003**, *19*, 6523−6533.
(54) Kaur, P.; Yue, H.; Wu, M.; Liu, M.; Treece, J.; Waldeck, D. H.; Xue, C.; Liu, H. Solvation and Aggregation of Polyphenylethynylene Based Anionic Polyelectrolytes in Dilute Solutions. *J. Phys. Chem. B* **2007**, *111*, 8589−8596.
(55) McQuade, D. T.; Kim, J.; Swager, T. M. Two-Dimensional Conjugated Polymer Assemblies: Interchain Spacing for Control of Photophysics. *J. Am. Chem. Soc.* **2000**, *122*, 5885−5886.
(56) Dong, L.; Shang, G.; Shi, J.; Zhi, J.; Tong, B.; Dong, Y. Effect of Substituent Position on the Photophysical Properties of Triphenylpyrrole Isomers. *J. Phys. Chem. C* **2017**, *121*, 11658−11664.


DOI: 10.1021/acs.macromol.8b02645
*Macromolecules* 2019, 52, 1663−1670

(57) Kim, J.; Swager, T. M. Control of Conformational and Interpolymer Effects in Conjugated Polymers. *Nature* **2001**, *411*, 1030−1034.
(58) Wu, M.; Kaur, P.; Yue, H.; Clemmens, A. M.; Waldeck, D. H.; Xue, C.; Liu, H. Charge Density Effects on the Aggregation Properties of Poly(*p*-phenylene-ethynylene)-Based Anionic Polyelectrolytes. *J. Phys. Chem. B* **2008**, *112*, 3300−3310.



DOI: 10.1021/acs.macromol.8b02645
*Macromolecules* 2019, 52, 1663−1670